Low doses of the food contaminant Deoxynivalenol trigger apoptosis and alter GnRH stimulation of gonadotroph cells

Guodong Cai[1,3†], Lingchen Yang[2,3†], Francis Marien-Bourgeois[3], Derek Boerboom[3], Gustavo Zamberlam[3] and Imourana Alassane-Kpembi [3*]

[1]College of Veterinary Medicine, Yangzhou University, Yangzhou 225009, Jiangsu, China.

[2]College of Veterinary Medicine, Hunan Agricultural University, Changsha 410128, Hunan, China.

[3]Department of Veterinary Biomedicine, Faculty of Veterinary Medicine, Université de Montréal, Saint-Hyacinthe H3T 1J4, Quebec, Canada

* Corresponding author. E-mail: Imourana.aalassane-kpembi@umontreal.ca

Contributing authors: 008400@yzu.edu.cn; lcyang@hunau.edu.cn

† These authors contributed equally to this work.

Abstract

The *Fusarium* mycotoxin Deoxynivalenol (DON) represents a significant threat to both human and animal health. It can cross the blood-brain barrier and disrupt cerebral functions. One of the main mechanisms underlying DON toxicity involves the activation of mitogen-activated protein kinases (MAPKs). Gonadotropin-Releasing Hormone (GnRH) stimulation of pituitary gonadotroph cells to release luteinizing hormone (LH) and follicle-stimulating hormone (FSH) triggers the MAPKs pathway too. Yet, no research investigated the endocrine-disrupting effects of DON on pituitary gonadotropins. To address this gap, our study investigated the effects of DON on gonadotroph cell viability, and its impact on the GnRH-stimulated secretion of FSH and LH, using the murine gonadotroph LβT2 cells. Our results uncovered that low-dose exposure to DON (1nM) significantly impairs viability in gonadotroph cells at both 24 and 48 h. Moreover, exposure to DON shows to induce membrane phosphatidylserine translocation without loss of membrane integrity, supporting a DON-induced cytotoxicity through apoptosis initiation. Furthermore, DON specifically inhibits GnRH-induced Erk

phosphorylation, while leaving p38 unaffected. Subsequent experiments with DON-treated LβT2 cells stimulated with GnRH showed a dose-dependent reduction in gene expression associated Gonadotropin-Releasing Hormone receptor (*GnRHr*), Luteinizing Hormone subunit beta (*LHβ*), and Glycoprotein Hormones, alpha subunit (*Cgα*), along with a reduction in LH production. Our findings underscore the induction of DON cytotoxicity through active apoptosis and its impact on LH secretion by inhibiting Erk phosphorylation within the MAPKs pathway. This research contributes to a better understanding of the neurotoxic effects of DON and establishes a foundation for further studies exploring the neuroendocrine impact of mycotoxins.

Keywords: DON; pituitary gland; LβT2 cells; MAPK signal pathway; FSH; LH

1. Introduction

Mycotoxins, as pervasive contaminants of foodstuffs, pose a substantial threat to both food security and human health. Among them, Deoxynivalenol (DON), produced by *Fusarium* fungi species, is one of the most prevalent raising global concern for health risk (Streit et al. 2012). Severe exposure to DON can cause symptoms such as diarrhea, vomiting, leukocytosis, hemorrhage, and even death in both humans and animals (Knutsen et al. 2017; Sobrova et al. 2010; Urbanek et al. 2018). Recent studies have indicated that DON induces neurotoxicity by breaching the blood-brain barrier, exerting a direct impact on the brain (Bonnet et al. 2012; Burger et al. 2004; Fæste et al. 2022). In male rats exposed to DON, serum testosterone concentrations decreased in a dose-related manner, while the follicle-stimulating hormone (FSH) and luteinizing hormone (LH) concentrations increased, suggesting that DON could act directly on the pituitary gland, or affect Leydig cells and subsequently the ability of Sertoli cells to produce inhibin (Sprando et al. 2005). The pituitary gonadotropins FSH and LH are crucial hormones governing gonadal development, steroid synthesis, and gamete maturation (Bosch et al. 2021).

At the cellular level, the primary mechanism of DON involves inhibiting protein and nucleic acid synthesis by binding to the ribosome and activating cellular kinases, including the mitogen-activated protein kinases (MAPKs) p38, c-Jun N-terminal kinase, and extracellular-signal-regulated kinase (Erk) (Mishra et al. 2014a). This mechanism, influences various signal transduction pathways, including those related to cell proliferation, stress, inflammation, differentiation, and apoptosis (Murphy and Blenis

56 2006).

57 MAPKs are also involved in the primary regulation of the transcription of the gonadotropins subunit
58 in the pituitary cells in response to stimulation by Gonadotropin-Releasing Hormone (GnRH)
59 (Kahnamouyi et al. 2018). Yet, no research explored the endocrine-disrupting effects of DON on pituitary
60 gonadotropins.

61 To address this gap, our study investigated the effects of DON on gonadotroph cell viability, and its
62 impact on the GnRH-stimulated secretion of FSH and LH, using the murine gonadotroph LβT2 cells.
63 The LβT2 cell line, derived from a pituitary tumor of mouse, has been reported to express and secrete
64 LH and FSH (Graham et al. 1999; Turgeon et al. 1996). This cell line serves as a crucial tool for the study
65 of gonadotroph physiology. This research offers scientific foundation to probe into DON's interference
66 with Gonadotropin secretion and the underlying mechanisms. Furthermore, it sets the stage for future
67 investigations into the reproductive impairments induced by DON, thereby establishing a more
68 comprehensive picture of its toxic mechanisms

69 **2. Materials and methods**

70 *2.1 Chemicals and Reagents*

71 DON and Dimethyl sulfoxide (DMSO) were obtained from Millipore Sigma Canada Ltd. (Ontario,
72 Canada). GnRH was from Peptide Pros (Miami, USA). Dulbecco's Modified Eagle's Medium (DMEM),
73 Fetal Bovine Serum (FBS), gentamycin and Trypsin were from Wisent (St-Bruno, Quebec, Canada).

74 *2.2 Cell culture*

75 After thawing, the mouse LβT2 gonadotroph-like cells were seeded in flasks and cultured in DMEM
76 medium (Wisent, St-Bruno, Quebec, Canada) supplemented with 10% FBS and 4 μg/mL gentamycin at
77 37°C with 5% CO_2 in the incubator. The culture medium was refreshed every two days after cellular
78 adhesion to the flask bottom was achieved.

79 *2.3 Cytotoxicity assessment*

80 LβT2 cells were distributed in 96-well plates at a density of 5×10^3 cells in 100 μL culture medium
81 per well and allowed to attach. The following day, the culture medium was aspirated, and the cells were
82 exposed to 100 μL of a new medium with graded concentrations of DON (0nM, 1nM, 10 nM, 10^2 nM,

83 10^3 nM and 10^4nM). Following 24 h of exposure to DON, CellTiter Blue (Promega, Madison, WI) was
84 performed as previously described by Cai et al. (2023).

85 *2.4 Real-time apoptosis and necrosis assay*

86 The Real Time-Glo™ Annexin V Apoptosis and Necrosis Assay (Promega, Madison, WI, Cat#:
87 JA1011) was used to simultaneously analyze apoptosis and necrosis. This assay probes the exposure of
88 phosphatidylserine on the outer leaflet of the cell membrane during apoptosis, while producing a
89 fluorescent signal upon the loss of membrane integrity, as a consequence of the binding of the cell-
90 impermeant pro-fluorescent DNA dye it contains.

91 LβT2 cells were seeded at a density of 3×10^4 cells per well in 100 μL culture medium in white clear-
92 bottom 96-well plates (Costar, Cambridge, MA, USA) and allowed to stabilized in a CO2 incubator..
93 After 48 h, 50 μL of the existing cell medium was carefully withdrawn and replaced by an equivalent
94 volume of fresh medium containing 40 nM DON. In each well, 100 μL of a 2X reagent solution was
95 dispensed, according to the manufacturer's instructions, resulting in a final liquid volume of 200 μL per
96 well. This ensured a final mycotoxin concentration of 10 nM in the well. Subsequently, the plates were
97 placed in a 37°C incubator with 5% CO2. Measurements were taken at 2 h, 6 h, and 24 h, to assess
98 membrane integrity through fluorescence (ex/em: 485 ± 10/525 ± 10), and phosphatidylserine
99 translocation through the luminescence signal generated by the Annexin V-dependent assembly of two
100 luciferase fragments.

101 *2.5 LβT2 Cell treatments for MAPK activation*

102 LβT2 cells were cultured for 24 hours in 24-well plates at a density of 1.5×10^5 cells in 300 μL of
103 medium per well. Then the cells were either directly stimulated with graded concentrations of GnRH
104 from 0.001nM to 0.1nM for 15 min, or pre-treated with DON at concentrations of 1 μM and 10 μM for
105 15 min, before stimulation with 0.1nM GnRH for 15 min. Following exposure, cellular proteins were
106 extracted using a radioimmunoprecipitation assay (RIPA) buffer. The protein concentrations of the
107 samples were quantified using a bicinchoninic acid (BCA) protein quantification kit from Thermo Fisher
108 Scientific (Waltham, Massachusetts, USA). Protein samples were separated using a Precast Midi Protein
109 Gel (BIO-RAD , Hercules, California, USA) and then transferred to polyvinylidene fluoride (PVDF)
110 membranes (BIO-RAD , Hercules, California, USA). Primary antibodies specific to phosphorylated Erk,

111 p38, total Erk, p38, and β-tubulin were applied. Detection was facilitated using a peroxidase-conjugated
112 secondary antibody (Jackson ImmunoResearch Inc, USA), and the antigen-antibody complexes were
113 visualized using an enhanced chemiluminescence assay (ECL, Invitrogen , Carlsbad, California, USA).

114 *2.5 LβT2 cell treatments for gene expression and gonadotropin release*

115 LβT2 cells were seeded and allowed to attach in 6-well plates at a density of 1×10^6 cells per well.
116 On the next day, the cell supernatant was carefully aspirated, and replaced with new culture medium with
117 graded concentrations of DON from 1 nM to 10 μM, for an exposure duration of 24 h. The cells were
118 then stimulated with 1nM GnRH for 6 h. Afterwards, medium was collected for LH measurement and
119 the cells harvested for total RNA extraction.

120 *2.6 Total RNA extraction and real-time PCR*

121 The expression of *GnRHr* encoding the GnRH receptor and the gonadotropin-related genes *CGα*,
122 *LHβ*, and *FSHβ* was analyzed.

123 Total RNA was extracted using Trizol as per the guidelines provided by the manufacturer (BIO-
124 RAD). Following purity and concentration check on a Nanodrop spectrophotometer, total RNA (1μg)
125 was reverse transcribed into cDNA, using ADVANCED CDNA SYNTHESIS KIT (Wisent Bioproducts,
126 St-Bruno, QC, Canada) according to the manufacturer's instructions.

127 RT-qPCR was run on a CFX96 Touch Real-Time PCR Detection System (BIO-RAD) using qPCR
128 Mastermix with Supergreen (Wisent Bioproducts, St-Bruno, QC, Canada) following the manufacturer's
129 protocol. To ensure specificity of PCR products, melting curve were analyzed and the amplicons were
130 sequenced to verify authenticity. Experimental samples were run in duplicate and data were expressed
131 relative to *Rpl19* as housekeeping gene, and normalized to a calibrator sample using the Pfaffl method
132 with correction for amplification efficiency (Pfaffl 2001). Primer details for both the target genes and the
133 housekeeping gene are provided in Table 1.

134 *2.6 LH measurement*

135 LH levels in cell culture medium samples were evaluated by the Ultra-Sensitive Mouse and Rat LH
136 ELISA performed by the Center for Research in Reproduction at the Ligand Assay and Analysis Core
137 Laboratory of the University of Virginia. The capture monoclonal antibody (anti-bovine LH beta subunit,

518B7; RRID:AB_2784498) is provided by Janet Roser, University of California. The detection polyclonal antibody (rabbit LH antiserum, AFP240580Rb; RRID:AB_2784499) is provided by the National Hormone and Peptide Program (NHPP). HRP-conjugated polyclonal antibody (goat anti-rabbit) is purchased from DakoCytomation (Glostrup, Denmark; D048701-2; RRID:AB_2784500). Mouse LH reference prep (AFP5306A; NHPP) is used as the assay standard. The Limit of Quantitation is 0.016 ng/ml.

2.7 Statistical analysis

All statistical analyses were performed with Prism software 8.0.2 for Windows (GraphPad). The reported values are the means ± standard error of the mean (SEM) of at least three independent experiments, each with triplicate wells per experimental condition. Data were transformed to logarithms if they were not normally distributed (Shapiro–Wilk test). Two-tailed *t* tests or one-way ANOVAs followed by Tukey's multiple-comparison tests were run for comparisons between the experimental conditions. Differences with a p value < 0.05 were considered statistically significant.

3 Results

3.1 Low concentrations of DON altered the viability of gonadotroph cells

Using the CellTiter-Blue® Cell Viability Assay,the cytotoxicity of DON for LβT2 cells was assessed (Fig. 1). Exposure to DON decreased the viability of LβT2 cells, becoming significant even at the lowest tested concentration of 1 nM after 24 h ($p<0.05$) and 48 h ($p<0.01$). The decline in cell viabilities demonstrated a clear dose-dependent pattern at both 24 and 48 h, reaching its nadir at 10^4 nM DON for both exposure durations ($p<0.01$). Furthermore, the results also indicated that with longer exposure times, the impact on the activity of LβT2 cells was more profound. This suggests a dose and time-dependent reduction in viabilities of LβT2 cells in response to DON.

3.2 DON induced apoptosis in gonadotroph cells

To further substantiate the mechanism of DON-induced cytotoxicity on LβT2 cells, we conducted a real-time assay aimed at elucidating the temporal dynamics of translocation of phosphatidylserine and loss of membrane integrity following exposure to the mycotoxin (Fig. 2). Translocation of phosphatidylserine to the outer leaflet of the plasma membrane is revealed through annexin V binding

165 coupled with a luminescent signal emission, while loss of membrane integrity is associated with a
166 fluorescent signal resulting from DNA staining by a cell-impermeant reagent. Apoptotic cell death is
167 distinguished by a temporal lag between phosphatidylserine translocation and the compromise of
168 membrane integrity, whereas necrotic cell death is characterized by simultaneous annexin V binding and
169 the disruption of membrane integrity.

170 At the 6-h exposure time point, 10 nM DON already significantly increased phosphatidylserine
171 translocation compared to the control ($p<0.01$), while no significant difference in membrane integrity
172 loss was observed ($p>0.05$). However, both phosphatidylserine translocation and membrane integrity
173 compromise showed statistically significant differences between 10 nM DON-treated cells and the
174 control at the 24-h exposure. This indicates that exposure to 10 nM DON for 6 h induced apoptosis
175 without triggering necrosis.

176 *3.3 Phosphorylation of Erk, but not p38, in GnRH-stimulated gonadotroph cells is attenuated by DON*

177 We investigated the effects of DON exposure on the activation of MAPKs by GnRH in gonadotroph
178 cells.

179 Prior to a 15-min exposure to different concentrations of GnRH, LβT2 cells were exposed or not to
180 1μM or 10μM DON. Figure 3 and figure 4 present protein expression and phosphorylation states of Erk
181 and p38 in LβT2 cells. These results indicate that 0.1 nM GnRH induced a significant phosphorylation
182 of Erk and p38 proteins ($p<0.001$). On the other hand, pre-treatment of LβT2 cells with DON dose-
183 dependently decreased phosphorylation of Erk by GnRH, while no significant effect of DON could be
184 observed for the phosphorylation of p38.

185 *3.4 GnRH activation of key-regulatory genes for gonadotropin release is impaired by DON*

186 Next, we investigated the effects of DON on GnRH activation of some of the genes considered
187 essential in the synthesis of gonadotropins, namely the gonadotropin subunit encoding genes *CGα*, *FSHβ*
188 and *LHβ*, and *GnRHr*, encoding the receptor that mediates the GnRH stimulation of the secretion of the
189 gonadotropic hormones.

190 In comparison with the control group, GnRH stimulation led to clear up-regulation of *GnRHr*, *CGα*,
191 and *LHβ* ($p < 0.001$, $p < 0.01$, $p < 0.05$), but not *FSHβ* ($p = 0.14$) (Fig. 5). By contrast, the GnRH

activation of *CGα* ($p < 0.001$), and *LHβ* ($p < 0.001$), but not *GnRHr,* was hindered in DON-exposed gonadotroph cells.

3.5 LH production in gonadotroph cells is dose-dependently inhibited by DON

To further evaluate the interference of DON o*n gonadotropin* release, we assessed LH production in LβT2 cells. Figure 6 presents LH concentration in the cell culture supernatant of LβT2 cells exposed to graded concentrations of DON. Stimulation of the gonadotroph cells with 1nM GnRH for 6 h markedly activate their LH production as anticipated. Exposure to DON induced a clear dose-dependent inhibition of LH production. This inhibition was significant from 1μM DON ($p<0.05$).

Discussion

This study provides clear evidence of the endocrine-disrupting effects of DON exposure on pituitary gonadotropins. We demonstrate that exposure to realistic concentrations of the type B trichothecene mycotoxin DON is cytotoxic to gonadotroph cells and alters their GnRH stimulation through inhibition of Erk phosphorylation within the MAPKs pathway.

A growing body of literature is pointing to the impact of *Fusarium* mycotoxins on the hypothalamic–pituitary–gonadal (HPG) axis. The type A trichothecene mycotoxin T-2 was reported to induce alterations upstream in the rat HPG axis, through increase of hypothalamic GnRH synthesis, and downstream through precocious onset of the pubertal development of reproductive organs (Yang et al. 2016). Downstream of the HPG axis, the type B trichothecene DON has demonstrated a negative impact on bovine granulosa cell steroidogenesis and survival (Guerrero-Netro et al. 2015). In rat, DON also increased progenitor Leydig cell proliferation but inhibited their maturation and function, including steroidogenesis (Yang et al. 2024). Only few studies have investigated the toxicity of mycotoxins midstream of the HPG axis. DON induced growth inhibition of rat pituitary GH3 cells (Liu et al. 2020). In porcine gonadotroph cells, the *Fusarium* toxins ZEA and α-ZOL specifically inhibited FSH synthesis and secretion, but not LH (He et al. 2018). This FSH inhibiting effect relied on the activation of the membrane estrogen receptor GPR30, and subsequent phosphorylation of Protein kinase C (PKC), ERK and p38MAPK. GnRH regulates reproduction via binding a G-protein coupled receptor on the surface of the gonadotroph, through which it transmits signals, mostly via the MAPK cascade, to increase synthesis of LH and FSH (Melamed et al. 2012). One of the main mechanisms underlying DON toxicity involves

the activation of MAPKs (Payros et al. 2016). Most studies have reported a rapid increase in phosphorylation of JNK, ERK and p38 proteins in various cell types following exposure to DON (Lee et al. 2019; Mishra et al. 2014b; Zhang et al. 2020). However, the level of phosphorylated ERK decreased with increasing DON concentrations in piglet hippocampal nerve cells, indicating that the pattern of regulation of MAPKs may vary with cell types (Wang et al. 2018). Since both DON and GnRH activate the pivotal MAPKs for gonadotropin synthesis and release, we were interested to identify, midstream in the HPG axis, interference if any in GnRH stimulation of gonadotropin production that could result from gonadotroph cell exposure to DON.

We observed a significant decrease of the viability of the mouse gonadotroph cells even at the lowest tested concentration (1nM) of DON. Similar to the death mechanisms we previously reported in the intestinal mucosa, the cytotoxicity of DON toward the gonadotroph cells appeared clearly to be driven by apoptosis (Payros et al. 2021). These observations are relevant for several reasons. First, *in vivo* experiments have established that the transport of DON across the blood-brain barrier is effective, with the toxin being detected in the brain within minutes of oral exposure (Behrens et al. 2015; Prelusky et al. 1990), which means that the tiny population of gonadotroph cells that constitute only 7% to 15% of the total number of anterior pituitary cells are not protected from being exposed to dietary DON. Considering the provisional maximum tolerable daily intake (PMTDI), and the higher range of the exposure in adult and children to DONestablished by the Joint FAO/WHO Expert Committee on Food Additives, it is anticipated that the concentration of DON in the cerebrospinal fluid will be 0.45 to 1.08 nM (Maresca 2013). DON has been highlighted as of significant risk to human health, owing to the less than 30 safety factor between the doses of this mycotoxin susceptible to be present in the organism, in relation to its provisional maximum tolerable daily intake (PMTDI), and the doses affecting cell functions (Maresca and Fantini 2010; Muri et al. 2009). The 1 to 10 nM DON concentration range in this study showed clear cytotoxicity to LβT2 cells. Assuming that human gonadotroph cells have similar sensitivity to DON, the safety factor would be 0.9 to 20, positioning the pituitary as a prominent target for DON.

We observed that exposure of gonadotroph cells to DON prior to stimulation by GnRH decreases the phosphorylation level of Erk, but not p38. DON regulate MAPKs via the ribotoxic stress response, which involves the double-stranded RNA-activated protein kinase (PKR) and hemoitopoeitic cell kinase (Hck) as upstream transducers (Pestka 2008). Instead of PKR and Hck, GnRH activation of the

phosphorylation of Erk and p38-MAPKs is mediated by several isoforms of PKC (Harris et al. 1997; Maccario et al. 2004). Moreover, the profile of the PKC isoforms involved in GnRH to p38MAPK phosphorylation differs from ERK1/2 activation. On top of the PKCβII, PKCδ and PKCε isoforms reported for GnRH activation of the phosphorylation of Erk in LβT2 cells, the GnRH to p38MAPK phosphorylation also involves PKCα (Mugami et al. 2018). Our results suggest that, contrary to PKCβII, PKCδ and PKCε, the activation of MAPKs by GnRH via PKCα may escape interference with DON. This hypothesis deserves to be investigated.

The DON alteration of GnRH-induced phosphorylation of MAPKs in this study was paralleled by impaired activation of key-regulatory genes for gonadotropin release, and dose-dependent inhibition of the production of LH but not FSH by gonadotroph cells. However, it would be inaccurate to conclude that DON had no effect on FSH secretion, since the experimental design of our study was specifically tailored for LH secretion rather than FSH. Although produced in same gonadotroph cell, the release of LH or FSH depends on specific GnRH pulsality, with LH release favored by fast GnRH pulse frequencies and FSH favored by slow pulse frequencies (Tsutsumi and Webster 2009). To allow simultaneous release of FSH and LH, mouse pituitary cells were pulsed for 2 minutes at a 10 nM GnRH peak pulse concentration with a 58-minute interpulse interval for 4 hours (Kim and Lawson 2015), which is drastically different from the 0.1 to 1 nM GnRH stimulation for 15 minutes or six hours used in the present study. Further investigations featuring the suitable pulsality are needed to clarify the mechanisms involved in DON alteration of gonadotropin release.

In conclusion, our study uncovered the interference of DON on the release of gonadotropin in gonadotroph cells. We found that even low-dose DON can induce cytotoxicity of gonadotroph cells through apoptosis. Additionally, DON has a direct effect on the inhibition of gene expression relating to gonadotropin release and LH production, specifically by targeting the Erk phosphorylation within the MAPKs pathway. This research broadened our knowledge of DON's neurotoxic effects and brought a new depth to the potential neuroendocrine implications. This highlights the critical role of DON in compromising overall health, particularly its detrimental effects on the reproductive system, not only through direct effects on respective organs but also through interference with hormone secretion. This provides novel insights and considerations for elucidating the toxicological mechanisms of DON.

Acknowledgments:

The authors thank the University of Virginia Ligand Core that provided assistance in LH measurement in cell supernatant. The University of Virginia Center for Research in Reproduction Ligand Assay and Analysis Core that is supported by the Eunice Kennedy Shriver NICHD/NIH Grant R24HD102061

Funding: *This work was supported by Foundation J. Louis Lévesque. Lingchen Yang and Guodong Cai received a scholarship from China Scholarship Council.*

Financial interests: *Authors declare they have no financial interests.*

Author Contributions: *All authors contributed to the study conception and design. Conceptualization, Methodology and Funding acquisition* were performed by *Imourana Alassane-Kpembi; Formal analysis, Investigation, Data curation and Writing—original draft preparation* were performed by *Guodong Cai and Lingchen Yang; Writing—review and editing was performed by Francis Marien-Bourgeois and Derek Boerboom Visualization; Super-vision was performed by Imourana Alassane-Kpembi and Gustavo Zamberlam. All authors read and approved the final manuscript.*

Conflicts of Interest: *The authors declare no conflict of interest.*

References

Behrens M, Hüwel S, Galla HJ, Humpf HU (2015) Blood-Brain Barrier Effects of the Fusarium Mycotoxins Deoxynivalenol, 3 Acetyldeoxynivalenol, and Moniliformin and Their Transfer to the Brain. PloS one 10(11):e0143640 doi:10.1371/journal.pone.0143640

Bonnet MS, Roux J, Mounien L, Dallaporta M, Troadec J-D (2012) Advances in Deoxynivalenol Toxicity Mechanisms: The Brain as a Target. 4(11):1120-1138 doi:doi.org/10.3390/toxins4111120

Bosch E, Alviggi C, Lispi M, et al. (2021) Reduced FSH and LH action: implications for medically assisted reproduction. Human reproduction (Oxford, England) 36(6):1469-1480 doi:10.1093/humrep/deab065

Burger LL, Haisenleder DJ, Dalkin AC, Marshall JC (2004) Regulation of gonadotropin subunit gene transcription. J Mol Endocrinol 33(3):559-84 doi:doi.org/10.1677/jme.1.0160

Fæste CK, Solhaug A, Gaborit M, Pierre F, Massotte D (2022) Neurotoxic Potential of Deoxynivalenol in Murine Brain Cell Lines and Primary Hippocampal Cultures. 14(1):48 doi:doi.org/10.3390/toxins14010048

Graham KE, Nusser KD, Low MJ (1999) LbetaT2 gonadotroph cells secrete follicle stimulating hormone (FSH) in response to active A. The Journal of endocrinology 162(3):R1-5 doi:10.1677/joe.0.162r001

Guerrero-Netro HM, Chorfi Y, Price CA (2015) Effects of the mycotoxin deoxynivalenol on steroidogenesis and apoptosis in granulosa cells. Reproduction (Cambridge, England) 149(6):555-61 doi:10.1530/rep-15-0018

Harris D, Reiss N, Naor Z (1997) Differential activation of protein kinase C delta and epsilon gene expression by gonadotropin-releasing hormone in alphaT3-1 cells. Autoregulation by protein kinase C. The Journal of biological chemistry 272(21):13534-40 doi:10.1074/jbc.272.21.13534

He J, Wei C, Li Y, et al. (2018) Zearalenone and alpha-zearalenol inhibit the synthesis and secretion of pig follicle stimulating hormone via the non-classical estrogen membrane receptor GPR30. Molecular and cellular endocrinology 461:43-54 doi:10.1016/j.mce.2017.08.010

Kahnamouyi S, Nouri M, Farzadi L, Darabi M, Hosseini V, Mehdizadeh A (2018) The role of mitogen-activated protein kinase-extracellular receptor kinase pathway in female fertility outcomes: a focus on pituitary gonadotropins regulation. Therapeutic advances in endocrinology and metabolism 9(7):209-215 doi:10.1177/2042018818772775

Kim T, Lawson MA (2015) GnRH Regulates Gonadotropin Gene Expression Through NADPH/Dual Oxidase-Derived Reactive Oxygen Species. Endocrinology 156(6):2185-99 doi:10.1210/en.2014-1709

Knutsen HK, Alexander J, Barregård L, et al. (2017) Risks to human and animal health related to the presence of deoxynivalenol and its acetylated and modified forms in food and feed. EFSA journal European Food Safety Authority 15(9):e04718 doi:10.2903/j.efsa.2017.4718

Lee JY, Lim W, Park S, Kim J, You S, Song G (2019) Deoxynivalenol induces apoptosis and disrupts cellular homeostasis through MAPK signaling pathways in bovine mammary epithelial cells. Environmental pollution (Barking, Essex : 1987) 252(Pt A):879-887 doi:10.1016/j.envpol.2019.06.001

Liu A, Hu S, Wu Q, et al. (2020) Epigenetic upregulation of galanin-like peptide mediates deoxynivalenol induced-growth inhibition in pituitary cells. Toxicology and applied

336 pharmacology 403:115166 doi:10.1016/j.taap.2020.115166
337 Maccario H, Junoy B, Poulin B, Boyer B, Enjalbert A, Drouva SV (2004) Protein kinase Cdelta as
338 gonadotropin-releasing hormone target isoenzyme in the alphaT3-1 gonadotrope cell line.
339 Neuroendocrinology 79(4):204-20 doi:10.1159/000078102
340 Maresca M (2013) From the gut to the brain: journey and pathophysiological effects of the food-
341 associated trichothecene mycotoxin deoxynivalenol. Toxins 5(4):784-820
342 doi:10.3390/toxins5040784
343 Maresca M, Fantini J (2010) Some food-associated mycotoxins as potential risk factors in humans
344 predisposed to chronic intestinal inflammatory diseases. Toxicon : official journal of the
345 International Society on Toxinology 56(3):282-94 doi:10.1016/j.toxicon.2010.04.016
346 Melamed P, Savulescu D, Lim S, et al. (2012) Gonadotrophin-releasing hormone signalling
347 downstream of calmodulin. Journal of neuroendocrinology 24(12):1463-75
348 doi:10.1111/j.1365-2826.2012.02359.x
349 Mishra S, Dixit S, Dwivedi PD, Pandey HP, Das M (2014a) Influence of temperature and pH on the
350 degradation of deoxynivalenol (DON) in aqueous medium: comparative cytotoxicity of DON
351 and degraded product. Food additives & contaminants Part A, Chemistry, analysis, control,
352 exposure & risk assessment 31(1):121-31 doi:doi.org/10.1080/19440049.2013.861613
353 Mishra S, Tripathi A, Chaudhari BP, Dwivedi PD, Pandey HP, Das M (2014b) Deoxynivalenol induced
354 mouse skin cell proliferation and inflammation via MAPK pathway. Toxicology and applied
355 pharmacology 279(2):186-97 doi:10.1016/j.taap.2014.06.003
356 Mugami S, Dobkin-Bekman M, Rahamim-Ben Navi L, Naor Z (2018) Differential roles of PKC isoforms
357 (PKCs) in GnRH stimulation of MAPK phosphorylation in gonadotrope derived cells.
358 Molecular and cellular endocrinology 463:97-105 doi:10.1016/j.mce.2017.04.004
359 Muri SD, van der Voet H, Boon PE, van Klaveren JD, Brüschweiler BJ (2009) Comparison of human
360 health risks resulting from exposure to fungicides and mycotoxins via food. Food and
361 chemical toxicology : an international journal published for the British Industrial Biological
362 Research Association 47(12):2963-74 doi:10.1016/j.fct.2009.03.035
363 Murphy LO, Blenis J (2006) MAPK signal specificity: the right place at the right time. Trends in
364 biochemical sciences 31(5):268-75 doi:10.1016/j.tibs.2006.03.009
365 Payros D, Alassane-Kpembi I, Laffitte J, et al. (2021) Dietary Exposure to the Food Contaminant
366 Deoxynivalenol Triggers Colonic Breakdown by Activating the Mitochondrial and the Death
367 Receptor Pathways. Molecular nutrition & food research 65(23):e2100191
368 doi:10.1002/mnfr.202100191
369 Payros D, Alassane-Kpembi I, Pierron A, Loiseau N, Pinton P, Oswald IP (2016) Toxicology of
370 deoxynivalenol and its acetylated and modified forms. Archives of toxicology 90(12):2931-
371 2957 doi:10.1007/s00204-016-1826-4
372 Pestka JJ (2008) Mechanisms of deoxynivalenol-induced gene expression and apoptosis. Food
373 Additives & Contaminants: Part A 25(9):1128-1140 doi:10.1080/02652030802056626
374 Pfaffl MW (2001) A new mathematical model for relative quantification in real-time RT-PCR. Nucleic
375 acids research 29(9):e45 doi:10.1093/nar/29.9.e45
376 Prelusky DB, Hartin KE, Trenholm HL (1990) Distribution of deoxynivalenol in cerebral spinal fluid
377 following administration to swine and sheep. Journal of environmental science and health
378 Part B, Pesticides, food contaminants, and agricultural wastes 25(3):395-413
379 doi:10.1080/03601239009372697

380 **Sobrova P, Adam V, Vasatkova A, Beklova M, Zeman L, Kizek R (2010) Deoxynivalenol and its toxicity.**
381 **Interdisciplinary toxicology 3(3):94-9 doi:10.2478/v10102-010-0019-x**
382 **Sprando RL, Collins TF, Black TN, et al. (2005) Characterization of the effect of deoxynivalenol on**
383 **selected male reproductive endpoints. Food and chemical toxicology : an international**
384 **journal published for the British Industrial Biological Research Association 43(4):623-35**
385 **doi:10.1016/j.fct.2004.12.017**
386 **Streit E, Schatzmayr G, Tassis P, et al. (2012) Current Situation of Mycotoxin Contamination and Co-**
387 **occurrence in Animal Feed—Focus on Europe. 4(10):788-809**
388 **Tsutsumi R, Webster NJ (2009) GnRH pulsatility, the pituitary response and reproductive dysfunction.**
389 **Endocrine journal 56(6):729-37 doi:10.1507/endocrj.k09e-185**
390 **Turgeon JL, Kimura Y, Waring DW, Mellon PL (1996) Steroid and pulsatile gonadotropin-releasing**
391 **hormone (GnRH) regulation of luteinizing hormone and GnRH receptor in a novel**
392 **gonadotrope cell line. Molecular endocrinology (Baltimore, Md) 10(4):439-50**
393 **doi:10.1210/mend.10.4.8721988**
394 **Urbanek KA, Habrowska-Górczyńska DE, Kowalska K, Stańczyk A, Domińska K, Piastowska-Ciesielska**
395 **AW (2018) Deoxynivalenol as potential modulator of human steroidogenesis. 38(12):1450-**
396 **1459 doi:https://doi.org/10.1002/jat.3623**
397 **Wang X, Fan M, Chu X, et al. (2018) Deoxynivalenol induces toxicity and apoptosis in piglet**
398 **hippocampal nerve cells via the MAPK signaling pathway. Toxicon : official journal of the**
399 **International Society on Toxinology 155:1-8 doi:10.1016/j.toxicon.2018.09.006**
400 **Yang J, Ye L, Cui R, et al. (2024) Deoxynivalenol Inhibits Progenitor Leydig Cell Development by**
401 **Stimulating Mitochondrial Fission in Rats. Journal of agricultural and food chemistry**
402 **72(18):10616-10626 doi:10.1021/acs.jafc.4c01151**
403 **Yang R, Wang YM, Zhang L, Zhao ZM, Zhao J, Peng SQ (2016) Prepubertal exposure to T-2 toxin**
404 **advances pubertal onset and development in female rats via promoting the onset of**
405 **hypothalamic-pituitary-gonadal axis function. Human & experimental toxicology**
406 **35(12):1276-1285 doi:10.1177/0960327116629529**
407 **Zhang H, Deng X, Zhou C, Wu W, Zhang H (2020) Deoxynivalenol Induces Inflammation in IPEC-J2 Cells**
408 **by Activating P38 Mapk And Erk1/2. Toxins 12(3) doi:10.3390/toxins12030180**
409
410
411

412 Figure 1

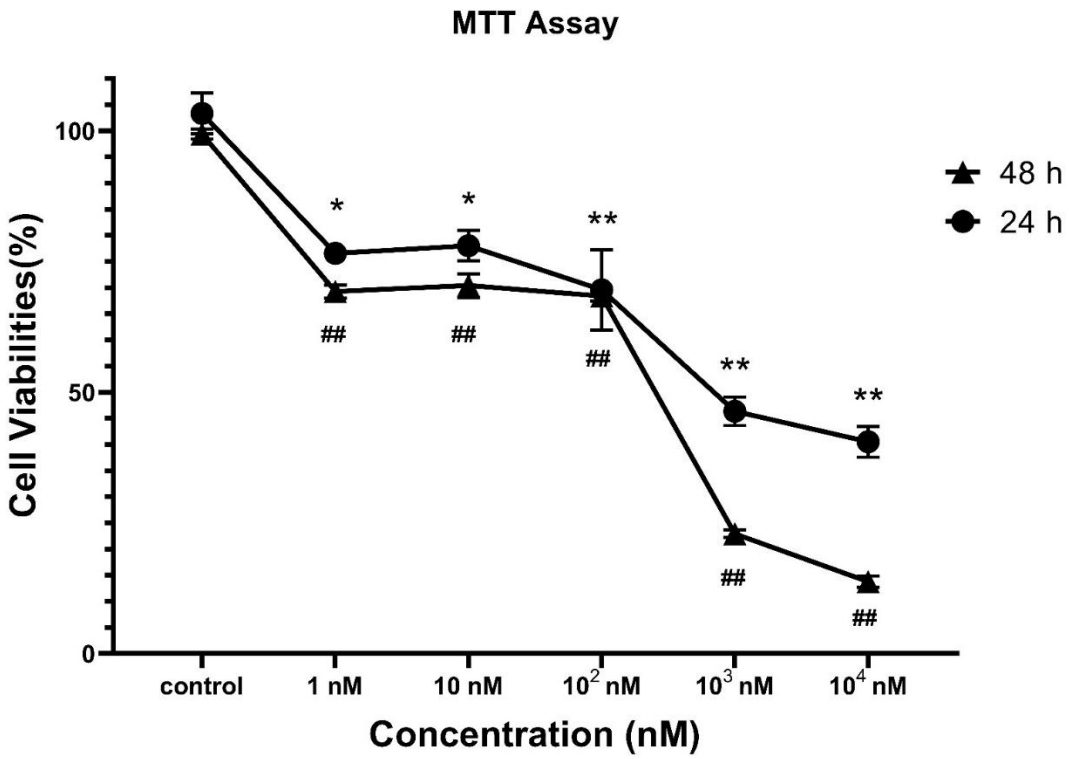

413

414

415 Figure 2

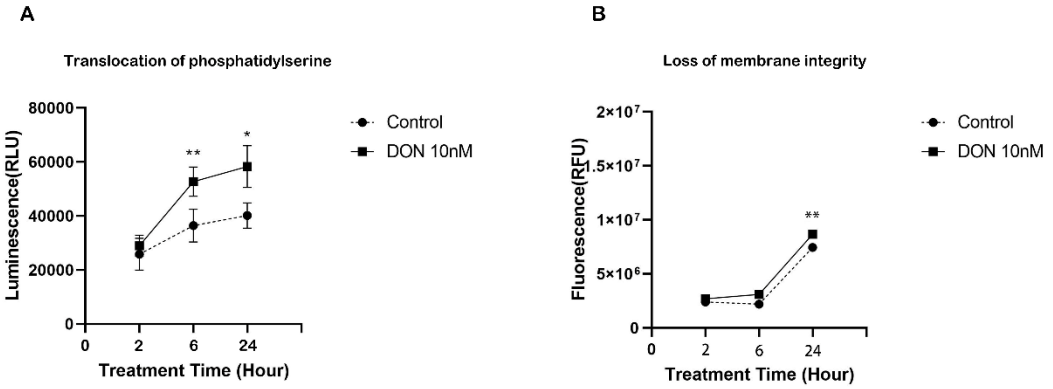

416
417

Figure 3

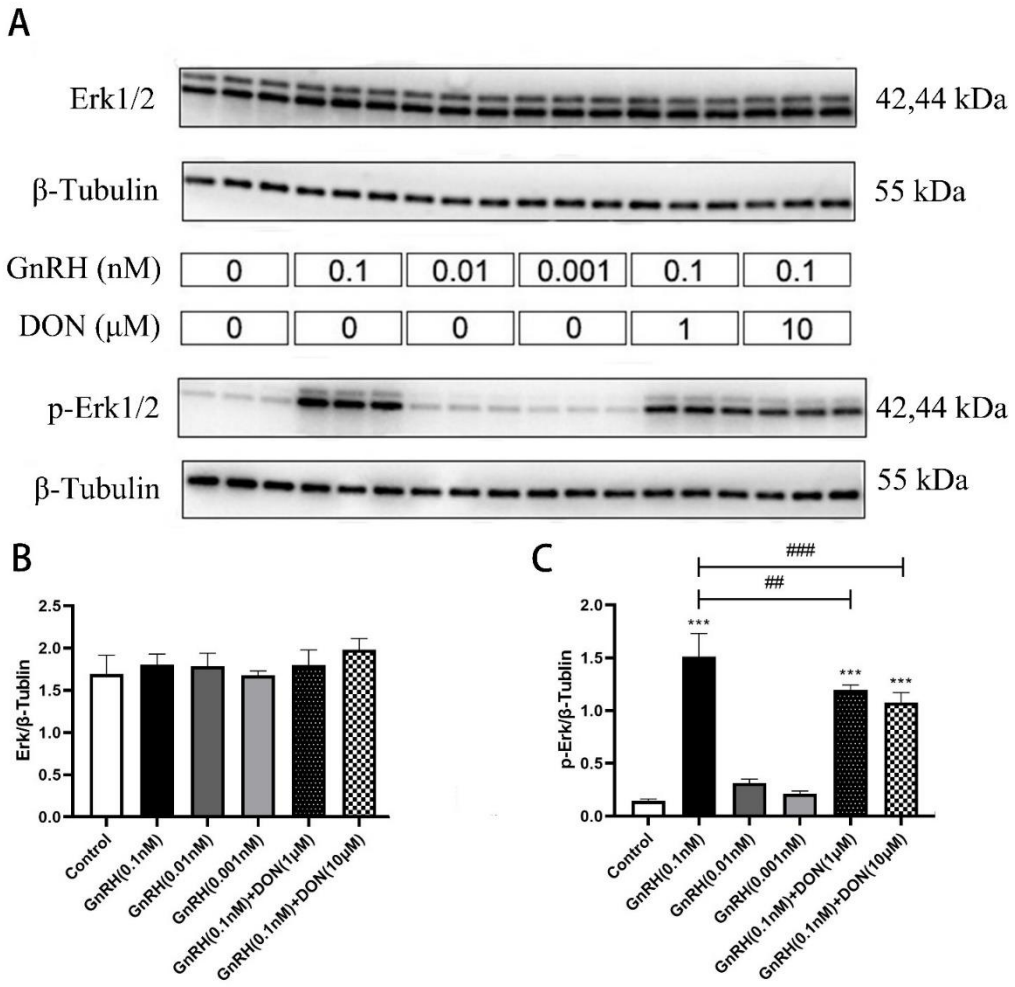
A
Erk1/2
42,44 kDa
β-Tubulin
55 kDa
GnRH (nM)
0
0.1
0.01
0.001
0.1
0.1
DON (μM)
0
0
0
0
1
10
p-Erk1/2
42,44 kDa
β-Tubulin
55 kDa
B
Erk/β-Tublin
2.5
2.0
1.5
1.0
0.5
0.0
Control
GnRH(0.1nM)
GnRH(0.01nM)
GnRH(0.001nM)
GnRH(0.1nM)+DON(1μM)
GnRH(0.1nM)+DON(10μM)
C
###
##
p-Erk/β-Tublin
2.0
1.5
1.0
0.5
0.0
***
***
***
Control
GnRH(0.1nM)
GnRH(0.01nM)
GnRH(0.001nM)
GnRH(0.1nM)+DON(1μM)
GnRH(0.1nM)+DON(10μM)

421 Figure 4

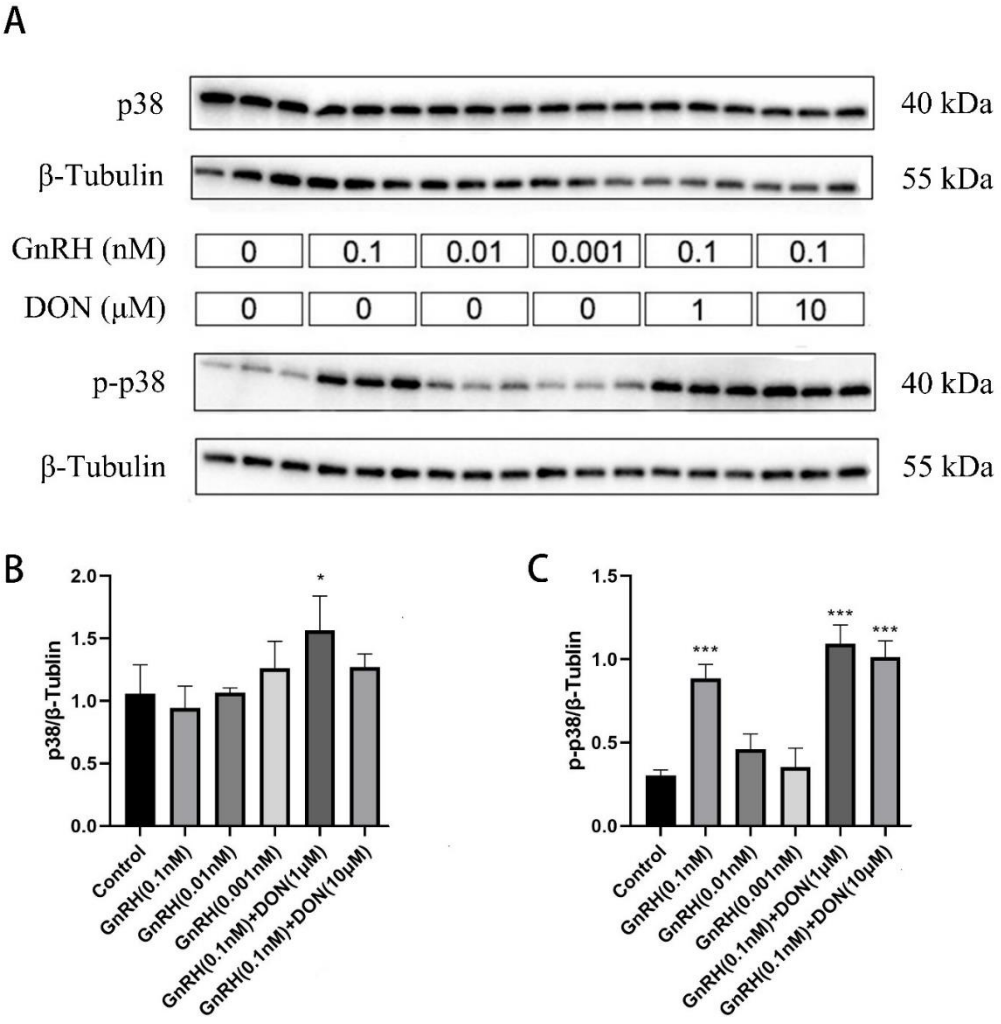

422

423

Figure 5

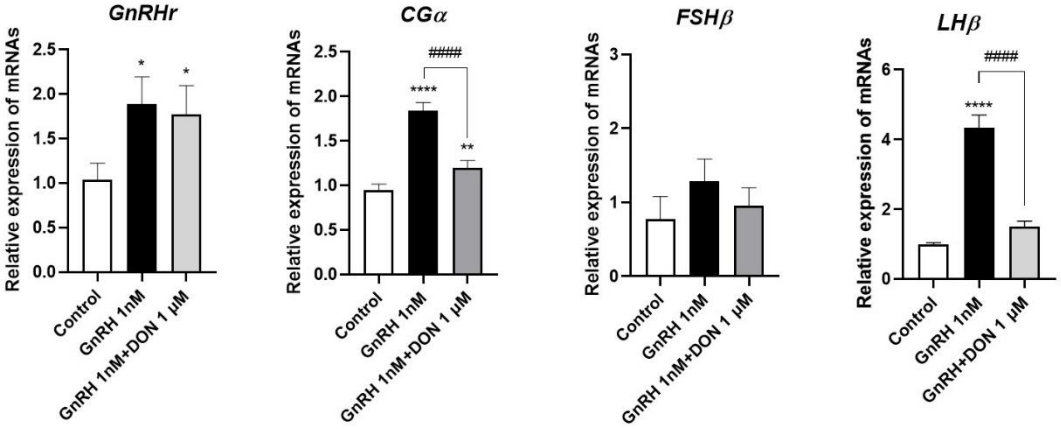
GnRHr
CGα
FSHβ
LHβ
Relative expression of mRNAs
Control
GnRH 1nM
GnRH 1nM+DON 1 μM
GnRH+DON 1 μM
*
****
**
####

427 Figure 6

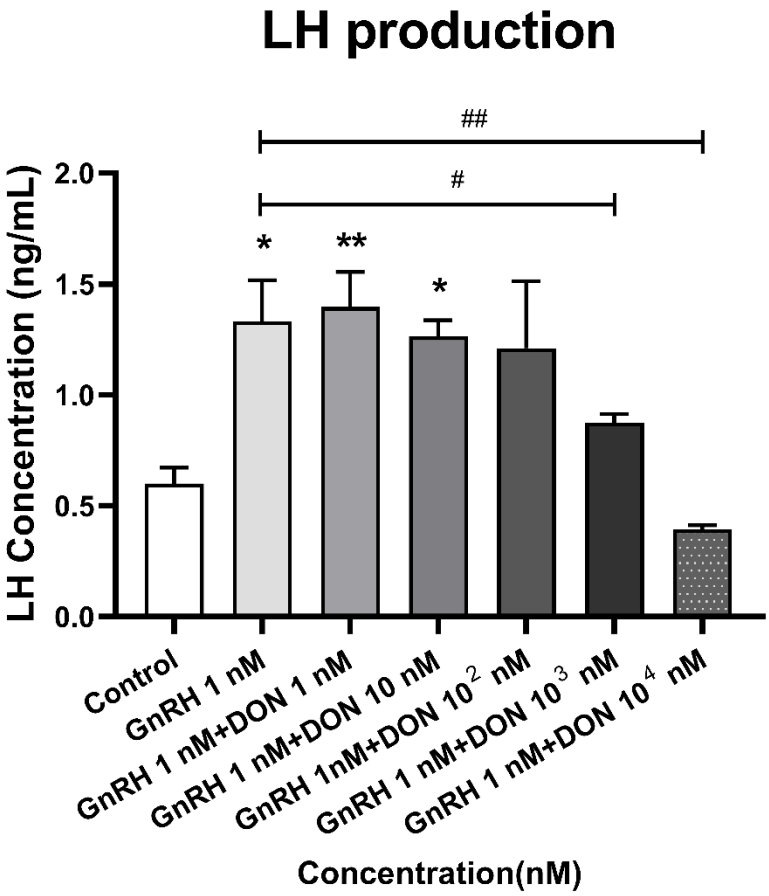

428

429 Table 1. Primer sequences of RT-qPCR

Gene	Upstream primers（5’→3’）	Downstream primers（5’→3’）
Rpl19	CTGAAGGTCAAAGGGAATGTG	GGACAGAGTCTTGATGATCTC
FSHβ	GCTACTGCTACACTAGGGATCTGG	TGGTCCTTCAGGACAAGGGT
LHβ	ACTGTGCCGGCCTGTCAACG	AGCAGCCGGCAGTACTCGGA
GnRHr	TTCGCTACCTCCTTTGTCGT	CACGGGTTTAGGAAAGCAAA
CGα	TCCCTCAAAAAGTCCAGAGC	GAAGAGAATGAAGAATATGCAG

430

431